Accepted Manuscript

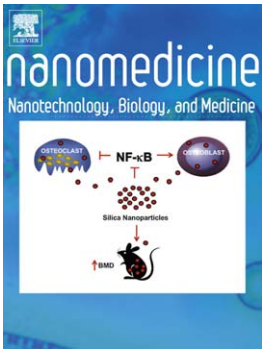

Retro-inverso peptide inhibitor nanoparticles as potent inhibitors of aggregation of the Alzheimer's Aβ peptide

Maria Gregori, Mark Taylor, Elisa Salvati, Francesca Re, Simona Mancini, Claudia Balducci, Gianluigi Forloni, Vanessa Zambelli, Silvia Sesana, Maria Michael, Christos Michail, Claire Tinker-Mill, Oleg Kolosov, Michael Scherer, Stephen Harris, Nigel J. Fullwood, Massimo Masserini, David Allsop

PII: S1549-9634(16)30176-9
DOI: doi: 10.1016/j.nano.2016.10.006
Reference: NANO 1448

To appear in: *Nanomedicine: Nanotechnology, Biology, and Medicine*

Received date: 6 August 2016
Revised date: 21 September 2016
Accepted date: 10 October 2016

Please cite this article as: Gregori Maria, Taylor Mark, Salvati Elisa, Re Francesca, Mancini Simona, Balducci Claudia, Forloni Gianluigi, Zambelli Vanessa, Sesana Silvia, Michael Maria, Michail Christos, Tinker-Mill Claire, Kolosov Oleg, Scherer Michael, Harris Stephen, Fullwood Nigel J., Masserini Massimo, Allsop David, Retro-inverso peptide inhibitor nanoparticles as potent inhibitors of aggregation of the Alzheimer's Aβ peptide, *Nanomedicine: Nanotechnology, Biology, and Medicine* (2016), doi: 10.1016/j.nano.2016.10.006

Retro-inverso peptide inhibitor nanoparticles as potent inhibitors of aggregation of the Alzheimer's Aβ peptide

Maria Gregori[a1], Mark Taylor[b1], Elisa Salvati[a], Francesca Re[a], Simona Mancini[a], Claudia Balducci[c], Gianluigi Forloni[c], Vanessa Zambelli[a], Silvia Sesana[a], Maria Michael[b], Christos Michail[b], Claire Tinker-Mill[b], Oleg Kolosov[d], Michael Scherer[b], Stephen Harris[e], Nigel, J. Fullwood[b], Massimo Masserini[a] and David Allsop[b*]

[a]University of Milano-Bicocca, Nanomedicine Center NANOMIB and School of Medicine and Surgery, Via Cadore, 48, 20900 Monza (MB), Italy.

[b]University of Lancaster, Division of Biomedical and Life Sciences, Faculty of Health and Medicine, Lancaster LA1 4YQ, UK.

[c]Department of Neuroscience, Istituto di Ricovero e Cura a Carattere Scientifico/Mario Negri Institute for Pharmacological Research, 20156 Milan, Italy.

[d]University of Lancaster, Department of Physics, Faculty of Science and Technology, Lancaster LA1 4YB, UK.

[e]Quotient Bioresearch (Rushden) Ltd, Pegasus Way, Crown Business Park, Rushden, Northamptonshire, NN10 6ER, UK.

[1]Maria Gregori and Mark Taylor contributed equally to this paper.

*Corresponding author at: University of Lancaster, Division of Biomedical and Life Sciences, Lancaster LA1 4YQ, UK. E-mail address: d.allsop@lancaster.ac.uk (D. Allsop)

The research leading to these results has received funding from the European Community's Seventh Framework Programme (FP7/2007-2013) under grant agreement n° 212043, and

from The Alzheimer's Society UK (grant number 210 (AS-PG-2013-032). There were also contributions from Lancaster University's Defying Dementia campaign.

Word Count	Abstract = 150	Complete manuscript = 5000
	Number of references = 41	Number of figures/tables = 8

Competing interests

The University of Lancaster has filed a patent (WO2013054110) on intellectual property related to this work, based on inventions of DA and MT. The patent has been licensed to MAC Clinical Research, UK.

Abstract

Aggregation of Amyloid-β peptide (Aβ) is a key event in the pathogenesis of Alzheimer's disease (AD). We investigated the effects of nanoliposomes decorated with the retro-inverso peptide RI-OR2-TAT (Ac-rGffvlkGrrrrqrrkkrGy-NH_2) on the aggregation and toxicity of Aβ. Remarkably low concentrations of these peptide inhibitor nanoparticles (PINPs) were required to inhibit the formation of Aβ oligomers and fibrils *in vitro*, with 50% inhibition occurring at a molar ratio of ~1:2000 of liposome-bound RI-OR2-TAT to Aβ. PINPs also bound to Aβ with high affinity (K_d = 13.2 - 50 nM), rescued SHSY-5Y cells from the toxic effect of pre-aggregated Aβ, crossed an *in vitro* blood-brain-barrier model (hCMEC/D3 cell monolayer), entered the brains of C57/BL6 mice, and protected against memory loss in APP_{SWE} transgenic mice in a novel object recognition test. As the most potent aggregation inhibitor that we have tested so far, we propose to develop PINPs as a potential disease-modifying treatment for AD.

Keywords: Alzheimer's disease, liposomes, retro-inverso peptide, β-amyloid, oligomer.

Background

There are currently ~36 million sufferers of Alzheimer's disease (AD) worldwide, costing the world economy US$604 billion in 2010, and these figures are set to rise dramatically in the future.[1] Current drug treatments only temporarily alleviate the symptoms of AD. Characteristic pathological changes of the disease are the presence of abundant senile plaques, containing Amyloid-β peptide (Aβ) fibrils, and neurofibrillary tangles consisting of hyperphosphorylated Tau protein. However, Aβ oligomers are now thought to be the most toxic form of this peptide, with a potent ability to cause memory deficits and inhibition of oligomer formation is a potential strategy for disease modification therapy.[2-8] It is also generally thought that Tau aggregation is a downstream consequence of Aβ aggregation.[9] The most advanced clinical trials aimed at disease modification in AD are based on drugs targeting the production or clearance of Aβ.[10]

We have published data on a small peptide (OR2 = H_2N-RGKLVFFGR-NH_2) that inhibits the formation of Aβ oligomers and fibrils.[11] RI-OR2 is a much more stable retro-inverted version of this peptide.[12] The addition of retro-inverted 'TAT' (HIV cell-penetrating peptide) to RI-OR2 allows it to enter cells and cross the blood-brain barrier (BBB).[13] Treatment of APPswe/PS1ΔE9 transgenic mice with RI-OR2-TAT caused reduction of brain Aβ burden (oligomers included), reduction of numbers of activated microglial cells, and an increase in the number of young neurons in the dentate gyrus.[13] However, RI-OR2-TAT only inhibits Aβ aggregation when present at relatively high concentrations (i.e. 1:5 molar ratio of inhibitor: Aβ at best).[13]

In recent years, there has been a growing interest in the use of liposomes as carriers for therapeutic agents, because of their attractive characteristics, such as biocompatibility, biodegradability, and chemical and physical stability.[14] Moreover, liposomes can be multi-functionalized on their surface, and it has been shown that multi-ligand-decorated

nanosystems can be more efficient (compared to single ligand systems) at recognizing their molecular targets.[15] In the present study, we have covalently attached RI-OR2-TAT to nanoliposomes (NL) using 'click' chemistry. We show that very low concentrations of these peptide inhibitor nanoparticles (PINPs) were required to inhibit the aggregation of Aβ and to protect cultured SHSY-5Y cells from the toxic effect of pre-aggregated Aβ. Moreover, they were efficient at crossing an *in vitro* BBB model, entered the brains of healthy mice, and protected against memory loss in APP_{SWE} transgenic mice.

Methods

Materials

Chemical reagents and Sepharose 4B-CL were from Sigma-Aldrich. Bovine brain sphingomyelin (Sm), cholesterol (Chol) and 1,2-distearoyl-sn-glycero-3-phosphoethanolamine-N-[maleimide(polyethylene glycol)-2000] (mal-PEG-PE) were from Avanti Polar Lipids Inc., USA. [^{3}H]-Sm, [^{3}H]-propranolol, [^{14}C]-sucrose, Ultima Gold scintillation cocktail and solvable tissue solubilizer were from PerkinElmer (Waltham, MA, USA). [^{14}C]-Chol was provided by Quotient Bioresearch Ltd. Polycarbonate filters for liposome extrusion were from Millipore Corp., Bedford, MA, USA and the extruder was from Lipex Biomembranes, Vancouver, Canada. Recombinant Aβ1-42, Ultrapure, was from rPeptide, Bogart, Georgia, USA. All other chemicals were reagent grade.

Production of NL decorated with RI-OR2-TAT (PINPs) by click chemistry

NL were composed of Sm/Chol (1:1 molar ratio) mixed with 5 molar % of mal-PEG-PE. Lipids were resuspended in chloroform/methanol (2:1, v:v) and dried under a gentle stream of nitrogen. The resulting film was resuspended in PBS, pH 7.4, vortexed and extruded 10 times through a 100 nm pore polycarbonate filter under 20 bar nitrogen pressure,

at room temperature, to create UD (undecorated) liposomes. In order to covalently attach the peptide to these liposomes, an additional cysteine residue was incorporated at the C-terminus. NL were incubated with this peptide for 2 h at 37°C and then overnight at 4°C to obtain PINPs. To remove unbound peptide, the liposome suspension was passed through a Sepharose 4B-CL column (25 x 1 cm). The elution of PINPs was assessed by Dynamic Light Scattering (DLS) and the amount of peptide bound to liposomes was quantified by Bradford assay.[16] Phospholipid recovery was determined by the method of Stewart.[17]

NL characterization

The size and polydispersity of NL were measured at 25°C using a ZetaPlus particle sizer (Brookhaven Instruments Corporation, Holtsville, NY, USA). The particle size was assessed by DLS with a 652 nm laser, and polydispersity index was obtained from the intensity autocorrelation function of the light scattered at a fixed angle of 90°.

The NL were also analysed by use of a Nanosight machine (NanoSight Ltd, Minton Park, Amesbury, UK) with NL suspended in PBS, pH 7.4, and measured at 25˚C.

Aβ aggregation assays

These were performed using de-seeded $A\beta_{1-42}$.[12]

ThT assays were conducted in 384-well, clear-bottomed microtitre plates, with 25 µM $A\beta_{1-42}$, 15 µM ThT, and a range of concentrations of PINPs, in 10 mM PBS, pH 7.4, with a total reaction volume of 60 µL. Aggregation was monitored using a BioTek Synergy plate reader (λ_{ex}=442 nm, λ_{em}=483 nm) over 48 h at 30°C, with the plate being shaken and read every 10 min. The results show average data from one of two experiments, each of which was performed in triplicate. Control assays involving incubation of pre-aggregated Aβ (incubated

at 25 μM for 24 h) with ThT in the presence of each inhibitor ruled out the possibility that the inhibitors interfere with binding of ThT to fibrils.[12]

For the sandwich immunoassay, Aβ oligomers were captured by monoclonal antibody 6E10 and detected by a biotinylated form of the same antibody.[12] Briefly, 96-well plates (Maxisorb) were coated with 6E10, diluted 1:1000 in assay buffer (Tris-buffered saline (TBS) (pH 7.4), containing 0.05% γ-globulins and 0.005% Tween 20). The incubated samples of peptide, with or without liposome (12.5 μM Aβ and a series of dilutions of PINPs in PBS, pH 7.4, at 25˚C), were diluted to 1 μM Aβ and incubated, in triplicate, in the 96-well plates for 1 h at 37˚C. The plates were washed with 10 mM PBS, containing 0.5% Tween 20 (PBS-T). Following this, 100 μL of TBS containing 1:1000 biotinylated 6E10 was added and the plates were incubated for 1 h at 37˚C and washed. Europium-linked streptavidin was added at 1:500 dilution in StrepE buffer (TBS containing 20 μM DTPA, 0.5% bovine serum albumin, and 0.05% γ-globulins), incubated for 1 h, and washed. Enhancer solution was added, and the plates were read on a Wallac Victor 2 plate reader. The results shown are average data from one of two experiments, each performed in triplicate. Pre-aggregated peptide controls ruled out the possibility that the inhibitors block binding of 6E10 to Aβ.[12]

Atomic force microscopy (AFM)

$A\beta_{1-42}$ was incubated at 25 μM in the presence or absence of 1.25 μM PINPs (total lipids) in PBS, pH 7.4, for 24 h. Samples were diluted 1:10 in PBS and a 2 μL aliquot was deposited onto a mica surface coated with poly-L-lysine (PLL)[18] and allowed to dry. Images were obtained in tapping mode using a Multimode™SPM NanoScope IIIa microscope (Digital Instruments, New York, USA). The silicon cantilever tips were 125 μm long, 30 μm wide and had a radius <10 nm (Budget Sensors, Bulgaria). The resonance frequency was 300 kHz and force constants 40 N/m. All images were first order flattened and edited using

WSxM 5.0 Develop 4.3 software, (Nanotech, Madrid, Spain).[19]

Electron microscopy (EM) studies of PINPs incubated with Aβ

Negative stain EM was used to examine the structure of PINPs with and without incubation with Aβ. PINPS alone, or PINPs (25 μM total lipids) incubated with $A\beta_{1-42}$ (25 μM) at 37°C for 48 h, were pipetted (4 μl) onto 300 mesh formvar and carbon coated copper grids (Agar Scientific, UK) and left for 1 min. The solvent was blotted away and the residue stained using 2% (w/v) phosphotungstic acid (PTA), pH 7.4. Immunogold labelling experiments were performed to identify any Aβ captured by PINPs. Here, the grids were blocked for 15 mins in goat serum:PBS (1:10) and incubated at room temperature for 1 h with primary anti-Aβ antibody 6E10 (0.02 μl/ml). After washing, they were incubated with 10 nm colloidal gold-conjugated goat anti-mouse secondary antibody (G7777, Sigma-Aldrich) diluted 1/50 in PBS, for 2 h. After washing, any liquid remaining on the grids was blotted away, and the samples were stained with PTA. Grids were left to dry and examined by TEM.

Surface plasmon resonance (SPR) spectroscopy

SPR experiments were conducted using a Sensi Q semi-automatic SPR machine (ICx Nomadics). This apparatus has two parallel flow cells; one was used to immobilize $A\beta_{1-42}$ monomers, oligomers or fibrils, while the other was used as "reference" (empty surface). A COOH5 sensor chip (ICx Nomadics) was employed for this purpose and the peptide was immobilized by amine coupling chemistry. Briefly, after surface activation, the peptide was diluted to 10 μM in acetate buffer (pH 4.0) and injected for 5 min at a flow rate of 30 μL/min. Any remaining activated groups were blocked with ethanolamine (pH 8.0). The final immobilization level was ~5000 resonance units (1 RU = 1 pg of protein/mm^2). The empty "reference" surface was prepared in parallel using the same immobilization procedure, but

without addition of peptide. Sensorgrams were obtained via injection of four different concentrations of PINPs (0.3 µM, 0.6 µM, 0.9 µM, 1.2 µM of exposed peptide) in solution (PBS with 0.005% Tween 20), over the immobilized ligand or control surface, in parallel, at the same time. These SPR data can be interpreted to provide an estimate for affinity of binding of liposomes to Aβ.[12,13]

MTS/LDH assay

Cultured SHSY-5Y human neuroblastoma cells were maintained in Dulbecco's Modified Eagle Medium (DMEM, Gibco) containing 10% Fetal Calf Serum, 100 U/mL penicillin, 50 µg/mL streptomycin, at 37ºC and 5% CO_2 in a humidified incubator. Cells were transferred to sterile 96-well growth plates at 20,000 cells per well and four wells per condition. For the effect of PINPs alone on cells, the growth medium was DMEM. Cells were left to adhere for 24 h before the PINPs were added and cell viability was assessed using the CellTiter 96AqueousOne Solution Cell Proliferation (MTS) Assay kit (Promega) after further 24 h incubation. For the experiments looking at the protective effect of PINPS, the growth medium was changed to Optimem (Invitrogen) and $A\beta_{1\text{-}42}$ that had been pre-aggregated (for 24 h at 25ºC in PBS) was added to a concentration of 5 µM. The plates were returned to the incubator for 24 h and cell proliferation was assessed as above.

Uptake and transcytosis of NL by human brain endothelial cells

Immortalized hCMEC/D3 were cultured as described previously.[20] 5×10^4 cells/cm^2 were seeded on 12-well transwell inserts coated with type I collagen and cultured with 0.5 mL and 1 mL of culture medium in the upper and lower chamber, respectively. Cells were treated with UD liposomes and PINPs when the transendothelial electrical resistance (TEER) value (measured by EVOMX meter, STX2 electrode; World Precision Instruments, Sarasota,

FL, USA) was found to be the highest. The functional properties of cell monolayers were assessed by measuring the endothelial permeability (EP) of [^{14}C]-sucrose and [^{3}H]-propranolol (between 0 and 120 mins) as described previously.[21] Radiolabeled NL (0.5 mL; 400 nmols/mL of total lipids) were added to the upper chamber and incubated for 120 min. After these periods of incubation, the radioactivity in the upper and lower chambers was measured by liquid scintillation counting to calculate the EP of NL across the cell monolayers, taking account of their passage through the filter without cells.[21] After 2 h, hCMEC/D3 cells were washed with PBS and detached from the transwell inserts with trypsin/EDTA for 15 mins at 37°C. Cell-associated radioactivity was measured and the total lipid uptake calculated.

Assessment of LIP cytotoxicity on hCMEC/D3 cells

hCMEC/D3 cells were grown on 12-well plates until confluence. Medium was replaced and NL (400 nmols/mL of total lipids) suspended in cell culture medium were incubated at 37°C with the cells for 24 h. After treatment, the cell viability was assessed by ([3-(4,5-dimethylthiazol-2-yl)-2,5-diphenyltetrazolium bromide]) (MTT) assay, as described previously.[22] Each sample was analyzed at least in triplicate. Moreover, TEER and permeability of [^{14}C]-sucrose were also determined in the presence of NL to assess the effect of NL on monolayer integrity.

Biodistribution in healthy mice

Three C57/BL6 male mice were administered with 0.4 mM (total lipid) of ^{14}C-labelled cholesterol PINPs, at ~2.22 x 10^{8} dpm/kg, into a tail vein. The amount of radioactivity that reached the brain was assessed by quantitative whole body analysis (QWBA), while the concentration in blood was measured by liquid scintillation counter from

samples taken prior to sacrifice. This work was performed by Quotient Bioresearch (Rushden) Ltd, using mice supplied by Charles Rivers UK Ltd., Margate, Kent.

Novel object recognition test in Tg mice

Drug and behavioral test naïve twenty-two-month-old Tg2576 (APP_{SWE}) and WT age-matched littermates were used. All experiments were conducted during the light cycle. Animals (Tg or WT) were injected intraperitoneally with PINPs (100 µl, 100 nmol of peptide/kg) or with PBS (100 µl) once a day for 21 days. The weight of the animals was monitored during treatment. Two experimental groups were treated with PINPs (Tg2576 and WT mice, n=10 for each), two control groups were treated with PBS (Tg2576 and WT, n=10 for each). In the NOR test, mice are introduced into an arena containing two identical objects that they can explore freely. Twenty-four hours later, mice are reintroduced into the arena containing the familiar object and a novel object. Exploration was recorded in a 10 min trial by an investigator blinded to the genotype and treatment and the time that each object was explored recorded. Results are expressed as percentage time of investigation on objects per 10 min, or as discrimination index (DI), i.e., (seconds spent on novel - seconds spent on familiar)/(total time spent on objects). Animals with no memory impairment spend a longer time investigating the novel object, giving a higher DI.

All procedures involving animals and their care were conducted according to EU laws and policies (EEC Council Directive 86/609, OJ L 358,1; 12 December 1987), the USDA Animal Welfare Act and NIH (Bethesda, MA, USA) policy on Humane Care and Use of Laboratory Animals. The procedures were reviewed and approved by the Mario Negri Institute Animal Care and Use Committee (1/04-D).

Results

Preparation and characterization of peptide inhibitor nanoparticles (PINPs)

To attach RI-OR2-TAT (Figure 1, A) covalently to the NL surface, we exploited a thiol-maleimide reaction employing an additional cysteine residue to provide the necessary thiol group.[23] This thiol function at the *C*-terminus of RI-OR2-TAT reacted with a maleimide-functionalized phospholipid present in the NL formulation (mal-PEG-PE) (Figure 1, B). The yield of coupling was 80-90% and, consequently, PINPs contained 2-2.5 mol% of peptide. The total lipid recovery of NL, after the reaction with the peptide and the purification step, was about 65%. Final preparations of PINPs were monodispersed, with a mean size of 143 ± 10 nm as determined by DLS. Their stability was verified by DLS which showed that the size and polydispersity index remained constant, in PBS, for up to 7 days. Analysis by a Nanosight instrument indicated an average size for PINPs of 131 ± 43 nm (Figure 1, C). AFM images showed NL particles with a mean diameter of ~100 nm (Figure 1, D), this slightly smaller size being most likely due to some dehydration of the sample.

Effects of PINPs on Aβ aggregation

RI-OR2-TAT alone was shown by ThT assay to inhibit $A\beta_{1-42}$ aggregation up to a molar ratio of 1:5 (inhibitor to $A\beta_{1-42}$), in agreement with previous data for RI-OR2 and RI-OR2-TAT[12,13]. When RI-OR2-TAT was attached to liposomes there was a dramatic improvement in ability to inhibit $A\beta_{1-42}$ fibril formation at low inhibitor concentrations (Figure 2, A). This finding is best illustrated in the dilution series shown in Figure 2, B. Here, it can be seen that 50% inhibition occurs at around 1:50 molar ratio of lipid to $A\beta_{1-42}$ or, as the inhibitory peptide is only ~2.5% of total lipids, ~1:2000 of RI-OR2-TAT to $A\beta_{1-42}$. In contrast, when UD liposomes (1:1) were tested for their ability to inhibit $A\beta_{1-42}$ aggregation,

we found a slight stimulatory effect at higher ratios of 1:1 and 1:2 (lipid:$A\beta_{1-42}$) but no effect below 1:10 (data not shown).

A sensitive immunoassay was used to detect Aβ oligomers present at the earlier $A\beta_{1-42}$ incubation time points (at around 4 h under our experimental conditions).[12,13] PINPs inhibited the generation of an immunoassay signal at all time points examined, and at molar ratios down to as low as 1:100 lipid:$A\beta_{1-42}$ or 1:4000 inhibitory peptide:$A\beta_{1-42}$ (Figure 2, C). The slight differences between ThT assay and ELISA results could reflect the fact that the former detects mainly fibrils, whereas the latter detects oligomers.

AFM images showed fibrils of $A\beta_{1-42}$ following 6 days of incubation in PBS (Figure 3, A) and when incubated with UD liposomes (Figure 3, B). Few or no fibrils were detected when PINPs were present at a molar ratio of 1:10 of total lipids:Aβ (Figure 3, C), confirming that they inhibit aggregation. However, some structures possibly resembling small aggregates could be seen, suggesting that PINPs may not entirely inhibit aggregation. Negative stain EM revealed that the surface of the PINPs was smooth and their shape was generally spherical. However, when the PINPs were incubated with $A\beta_{1-42}$ they appeared to be covered with a 'furry' coat of what are possibly Aβ monomers or oligomers (Figure 3, D). Intriguingly, some PINPs were found attached along the length of Aβ fibrils, and at their free ends, suggesting that the interaction of the PINPs had resulted in termination of fibril growth (Figure 3, D). Further investigation with anti-Aβ immunogold labelling showed that the surface of the PINPs was decorated with gold particles, confirming capture of Aβ (Figure 3, E).

Binding affinity between PINPs and Aβ

PINPs were injected over immobilized Aβ fibrils at different concentrations of RI-OR2-TAT (0.3, 0.6, 0.9, 1.2 μM) and were shown to bind in a concentration-dependent manner (Figure 4). Curves were fitted separately using the simplest Langmuir 1:1 interaction

model, and the calculated apparent affinity (k_d) was 36-50 nM. In addition, k_d values were 13.2 nM for Aβ oligomers and 22.5 nM for monomers (see Supplementary Information).

Effects of PINPs on the toxicity of Aβ

There was no loss in viability of SHSY-5Y cells, as measured by MTS assay, after 24 h incubation in the presence of PINPs at concentrations as high as 10 μM (total lipid) in normal (FCS supplemented DMEM) growth medium (Figure 5, A). A similar result was also found using the LDH cell viability assay (data not shown). Treatment of SHSY-5Y cells with 5 μM Aβ for 24 h gave a 39% reduction in cell viability, and the presence of PINPs rescued the cells from Aβ toxicity at all doses tested (Figure 5, B). UD liposomes were not toxic to neuroblastoma cells (Figure 5, A), and they did not rescue cells from the toxic effect of pre-aggregated Aβ (Figure 5, B).

Passage of PINPs across the blood-brain barrier

We measured the ability of PINPs to cross an artificial BBB model composed of a hCMEC/D3 cell monolayer.[24] hCMEC/D3 cells grown on transwell membrane inserts were incubated with UD liposomes or PINPs on day 12, when the maximal transendothelial electrical resistance (TEER) value was registered (123 ± 6 Ω · cm^2). Transport of [^{14}C]-sucrose and [^{3}H]-propranolol was measured, with paracellular EP values of 1.48×10^{-3} cm/min and 3.51×10^{-3} cm/min, respectively, in agreement with values reported in the literature.[25] Radiolabelled UD liposomes or PINPs were added in the upper compartment and the cellular uptake and EP were measured up to 2 h of incubation. The radioactivity stably associated with cells was 1.19 ± 0.32% and 4.19 ± 0.24% of the administered dose ($p<0.05$), respectively for UD liposomes and PINPs (Figure 6, A). Also the EP across the cell monolayers was higher for PINPs ($1.08 \pm 0.13 \times 10^{-4}$ cm/minute), compared to UD

liposomes ($2.25 \pm 0.89 \times 10^{-5}$ cm/minute) ($p<0.05$) (Figure 6, B). MTT assays showed that all of the preparations tested were nontoxic. Moreover, after hCMEC/D3 incubation with UD liposomes or PINPs, the TEER value and the permeability of [^{14}C]-sucrose ($119 \pm 8\ \Omega \cdot cm^2$ and 1.62×10^{-3} cm/minute, respectively) did not change, within experimental error (<3%).

Biodistribution of PINPs in healthy mice

QWBA measurements for biodistribution of PINPs are detailed in Table 1. Fifteen minutes after administration, 0.49%/g of the total dose was found in the brain and 0.952%/g in the blood, showing evidence for BBB penetration. However, the majority of the dose was found in lungs (~92%), and other tissues associated with phagocytosis by the mononuclear phagocyte system (i.e. adipose tissue, liver, bone marrow and spleen).

NOR (memory) test

Figure 7 shows that, although PBS-treated Tg2576 mice were unable to discriminate between the familiar and the novel object (percentage time of investigation per 10 min: familiar, 53.5 ± 1.5; novel, 46.5 ± 1.5; DI, -0.07 ± 0.03; n = 19), after treatment mice receiving PINPs significantly recovered their long term recognition memory (percentage time of investigation per 10 min: familiar, 40.4 ± 1.6; novel, 59.6 ± 1.6; DI, 0.19 ± 0.03; n = 10), close to the values of PBS-treated WT mice (percentage time of investigation per 10 min: familiar, 39.6 ± 1.4; novel, 60.4 ± 1.4; DI, 0.23 ± 0.02; n = 10) (One-way ANOVA, Tukey's post hoc test. *$p<0.05$). In addition, we demonstrated that treatment with PINPs had no negative effect on the memory of WT mice (percentage time of investigation per 10 min: familiar, 37.5 ± 4.7; novel, 62.5 ± 3.4; DI, 0.25 ± 0.09; n = 10) and did not affect mouse weight and motor activity (data not shown).

Discussion

Here, we linked RI-OR2-TAT covalently to the surface of NL composed of sphingomyelin and cholesterol. This lipid formulation has been widely utilized *in vivo* for therapeutic purposes and displays good blood circulation times, good biocompatibility, and high resistance to hydrolysis.[26] In addition, the 130-140 nm diameter is optimal for moving at an appreciable rate through the brain extracellular space.[27] We found that the presence of the carrier appears to increase the potency of RI-OR2-TAT as an aggregation inhibitor by 10-20 fold, where this is determined by the molar ratio of inhibitor:Aβ required to block the aggregation of Aβ1-42 under standard experimental conditions. We did not observe this phenomenon with curcumin-NL[28] and so it is not completely clear why there is this considerable jump in potency for PINPs compared to free peptide. However, creating multivalent peptide-dendrimers has been shown to increase the efficacy of a KLVFF peptide aggregation inhibitor[29] and this may be a factor in our study, due to several inhibitory peptides being able to interact simultaneously with oligomeric Aβ.

We reported previously a large increase in the affinity of RI-OR2-TAT for Aβ (K_d = 58-125 nM) compared to RI-OR2 alone (K_d = 9-12 μM), but this is not reflected in an equivalent jump in the ability of RI-OR2-TAT to inhibit Aβ aggregation at low concentrations of inhibitor.[12,13] We can conclude from this that an increase in binding affinity does not necessarily result in a more potent aggregation inhibitor. Here, we found that the affinity of PINPs for Aβ (K_d = 13.2-50 nM) is slightly higher than that obtained previously for RI-OR2-TAT, but the ability of PINPs to inhibit Aβ aggregation at low concentrations of the inhibitory peptide was greatly improved. In addition to multivalent interactions between RI-OR2-TAT and Aβ, another possible explanation for the potency of PINPs is based on the fact that RI-OR2-TAT contains many positively charged amino acid residues and the presence of multiple copies of this peptide on the NL surface (each PINP has around 1600

molecules of RI-OR2-TAT attached) would give a highly positively charged external layer that could attract and capture Aβ monomers, or oligomers as they form.[30] It is also feasible that Aβ is captured by the peptides exposed on the NL surface and is then incorporated into the lipid component of the NL, so effectively removing Aβ from solution. It is well known that Aβ oligomers insert into lipid membranes of cells and form pores or ion channels.[31-33]

The TAT portion of RI-OR-TAT, with its positively charged amino acid residues, also confers on the inhibitor an ability to cross the BBB and reach the brain.[13] Here we show that this ability is maintained for PINPs. The PE of NL, using the *in vitro* BBB model, was much higher for PINPs than for UD liposomes, proving the effectiveness of the functionalized NL to flux across the cellular monolayer. Moreover, some PINPs are transported into the brain, through the BBB of healthy mice, and they show a protective effect on memory loss in Tg2576 mice. It is also possible that this is due to the 'sink' effect with the liposomes rapidly binding Aβ in blood before being removed, and this is driving export of Aβ from the brain.

Other NP-based treatments for AD are under investigation, including antibody-coated NP and secretase inhibitors as well as our previously published curcumin and lipid-ligand linked NL[28,34-38] Despite promising preclinical data, no secretase inhibitor has succeeded in any advanced clinical trial[39] and, considering the serious side effects reported for immunisation with anti-Aβ antibodies[40], anti-Aβ-coated NP could be problematic. In contrast, PINPs have 'stealth' properties and so should not elicit any immune response. Moreover, the aggregation of Aβ seems to be a purely pathological phenomenon, and so inhibition of this process should not result in problematic side-effects.

In addition to these therapeutic implications, PINPs also have potential as a molecular imaging agent.[41] The high affinity of RI-OR2-TAT for Aβ should allow specific labeling of amyloid plaques, and possibly Aβ oligomers, through addition of a relevant contrast agent (CT/MRI) or radiolabel (PET/SPECT) to form a multifunctional NP with 'theranostic' utility.

References

1. Wimo A, Prince M. Alzheimer's Disease International World Alzheimer Report 2010 The Global Economic Impact of Dementia. Published by Alzheimer's Disease International (ADI) 21 September 2010.

2. Lambert MP, Barlow AK, Chromy BA, Edwards C, Freed R, Liosatos M, et al. Diffusible, nonfibrillar ligands derived from Aβ 1 42 are potent central nervous system neurotoxins. *Proc Natl Acad Sci USA* 1998;**95**:6448-53.

3. Wang HW, Pasternak JF, Kuo H, Ristic H, Lambert MP, Chromy B, et al. Soluble oligomers of β amyloid (1-42) inhibit long-term potentiation but not long-term depression in rat dentate gyrus. *Brain Res* 2002;**924**:133-40.

4. Walsh DM, Klyubin I, Fadeeva JV, Cullen WK, Anwyl R, Wolfe MS, et al. Naturally secreted oligomers of amyloid β protein potently inhibit hippocampal long-term potentiation in vivo. *Nature* 2002;**416**:535-39.

5. Kim HJ, Chae SC, Lee DK, Chromy B, Lee SC, Park YC, et al. Selective neuronal degeneration induced by soluble oligomeric amyloid β protein. *FASEB J* 2003;**17**:118-20.

6. Cleary JP, Walsh DM, Hofmeister JJ, Shankar GM, Kuskowski MA, Selkoe DJ, et al. Natural oligomers of the amyloid-β protein specifically disrupt cognitive function. *Nature Neurosci* 2005;**8**:79-84.

7. Walsh DM, Selkoe DJ. Aβ oligomers - a decade of discovery. *J Neurochem* 2007;**101**:1172-84.

8. Haass C, Selkoe DJ. Soluble protein oligomers in neurodegeneration: lessons from the Alzheimer's amyloid β-peptide. *Nature Rev Mol Cell Biol* 2007;**8**:101-12.

9. Ma Q-L, Yang F, Rosario ER, Ubeda OJ, Beech W, Gant DJ, et al. β-amyloid oligomers induce phosphorylation of tau and inactivation of insulin receptor substrate via c-Jun N-terminal kinase signaling: suppression by omega-3 fatty acids and curcumin. *J Neurosci* 2009;**29**:9078-89.

10. Howlett D. APP transgenic mice and their application to drug discovery. *Histol Histopathol* 2011;**26**:1611-32.

11. Austen BM, Paleologou KE, Ali SAE, Qureshi MM, Allsop D, El-Agnaf OMA. Designing peptide inhibitors for oligomerization and toxicity of Alzheimer's β-amyloid peptide. *Biochemistry* 2008;**47**:1984-92.

12. Taylor M, Moore S, Mayes J, Parkin E, Beeg M, Canovi M, et al. Development of a proteolytically stable retro-inverso peptide inhibitor of β amyloid oligomerization as a potential novel treatment for Alzheimer's disease. *Biochemistry* 2010;**49**:3261-72.

13. Parthsarathy V, McClean PL, Hölscher C, Taylor M, Tinker C, Jones G, et al. A novel retro-inverso peptide inhibitor reduces amyloid deposition, oxidation and inflammation and stimulates neurogenesis in the APPswe/PS1ΔE9 mouse model of Alzheimer's disease. *PLoS ONE* 2013;**8**:e54769.

14. Torchilin VP. Recent advances with liposomes as pharmaceutical carriers. *Nature Rev Drug Discov* 2005;**4**:145-60.

15. Stukel JM, Li RC, Maynard HD, Caplan MR. Two-step synthesis of multivalent cancer-targeting constructs. *Biomacromolecules* 2010;**11**:160-67.

16. Bradford MM. A rapid and sensitive method for the quantitation of microgram quantities of protein utilizing the principle of protein-dye binding. *Anal Biochem* 1976;**72**:248-54.

17. Stewart JCM. Colorimetric determination of phospholipids with ammonium ferrothiocyanate. *Anal Biochem* 1980;**104**:10-4.

18. Tinker-Mill C, Mayes J, Allsop D, Kolosov OV. Ultrasonic force microscopy for nanomechanical characterization of early and late-stage amyloid-β peptide aggregation. *Sci Rep* 2014;**4**:4004.

19. Horcas I, Fernández R, Gómez-Rodríguez JM, Colchero J, Gómez-Herrero J, Baro AM. WSXM: a software for scanning probe microscopy and a tool for nanotechnology. *Rev Sci Instrum* 2007;**78**:013705.

20. Re F, Cambianica I, Sesana S, Salvati E, Cagnotto A, Salmona M, et al. Functionalization with ApoE-derived peptides enhances the interaction with brain capillary endothelial cells of liposomes binding amyloid-β peptide. *J Biotechnol* 2010;**156**:341-6.

21. Cecchelli R, Dehouck B, Descamps L, Fenart L, Buée-Scherrer VV, Duhem C, et al. In vitro model for evaluating drug transport across the blood–brain barrier. *Adv Drug Deliv Rev* 1999;**36**:165-78.

22. Re F, Cambianica I, Zona C, Sesana S, Gregori M, Rigolio R, et al. Functionalization of liposomes with ApoE-derived peptides at different density affects cellular uptake and drug transport across a blood-brain barrier model. *Nanomedicine* 2011;**7**:551-9.

23. Nobs L, Zuchegger F, Gurny R, Allémann E. Current methods for attaching targeting ligands to liposomes and nanoparticles. *J Pharm Sci* 2004;**93**:1980-92.

24. Poller B, Gutmann H, Krähenbühl S, Weksler B, Romero I, Couraud PO, et al. The human brain endothelial cell line hCMEC/D3 as a human blood-brain barrier model for drug transport studies. *J Neurochem* 2008;**107**:1358-68.

25. Summerfield SG, Stevens AJ, Cutler L, del Carmen Osuna M, Hammond B, Tang SP, et al. Improving the in vitro prediction of in vivo central nervous system penetration: integrating permeability, P-glycoprotein efflux, and free fractions in blood and brain. *J Pharmacol Exp Ther* 2006;**316**:1282-90.

26. Webb MS, Harasym TO, Masin D, Bally MB, Mayer LD. Sphingomyelincholesterol liposomes significantly enhance the pharmacokinetic and therapeutic properties of vincristine in murine and human tumour models. *Br J Cancer* 1995;**72**:896-904.

27. Nance EA, Woodworth GF, Sailor KA, Shih TY, Xu Q, Swaminathan G, Xiang D, et al. A dense poly(ethylene glycol) coating improves penetration of large polymeric nanoparticles within brain tissue. *Sci Transl Med* 2012;4(149):149ra119. doi: 10.1126/scitranslmed.3003594.

28. Taylor M, Moore S, Mourtas S, Niarakis A, Re F, Zona C, et al. Effect of curcumin-associated and lipid ligand functionalised nanoliposomes on aggregation of the Alzheimer's Aβ peptide. *Nanomedicine* 2011;**7**:541-50.

29. Chafekar SM, Malda H, Merkx M, Meijer EW, Viertl D, Lashuel HA, et al. Branched KLVFF tetramers strongly potentiate inhibition of β-amyloid aggregation. *ChemBioChem* 2007;**8**:1857-64.

30. Wang Q, Shah N, Zhao J, Wang C, Zhao C, Liu L, et al. Structural, morphological, and kinetic studies of β-amyloid peptide aggregation on self-assembled monolayers. *Phys Chem Chem Phys* 2011;**13**:15200-10.

31. Arispe N, Rojas E, Pollard HB. Alzheimer disease amyloid β protein forms calcium channels in bilayer membranes: blockade by tromethamine and aluminum. *Proc Natl Acad Sci USA* 1993;**90**:567-71.

32. Arispe N, Pollard HB, Rojas E. Giant multilevel cation channels formed by Alzheimer disease amyloid β-protein [Aβ-(1–40)] in bilayer membranes. *Proc Natl Acad Sci USA* 1993;**90**:10573-77.

33. Fraser SP, Suh YH, Djamgoz MB. Ionic effects of the Alzheimer's disease β amyloid precursor protein and its metabolic fragments. *Trends Neurosci* 1997;**20**:67-72.

34. Richman M, Wilk S, Skirtenko N, Perelman A, Rahimipour S. Surface-modified protein microspheres capture amyloid-β and inhibit its aggregation and toxicity. *Chem Eur J* 2011;**17**:11171-7.

35. Gobbi M, Re F, Canovi M, Beeg M, Gregori M, Sesana S, et al. Lipid-based nanoparticles with high binding affinity for amyloid-β 1-42 peptide. *Biomaterials* 2010;**31**:6519-29.

36. Bana L, Minniti S, Salvati E, Sesana S, Zambelli V, Cagnotto A, et al. Liposomes bi-functionalized with phosphatidic acid and an ApoE-derived peptide affect Aβ aggregation features and cross the blood-brain-barrier: Implications for therapy of Alzheimer disease. *Nanomedicine* 2014;**10**:1583-90.

37. Canovi M, Markoutsa E, Lazar AN, Pampalakis G, Clemente C, Re F, et al. The binding affinity of anti-Aβ1-42 MAb-decorated nanoliposomes to Aβ1 42 peptides in vitro and to amyloid deposits in post-mortem tissue. *Biomaterials* 2011;**32**:5489-97.

38. Yoo SI, Yang M, Brender JR, Subramanian V, Sun K, Joo NE, et al. Mechanism of fibrillation inhibition of amyloid peptides by inorganic nanoparticles reveals functional similarities with proteins. *Angew Chem Int Ed* 2011;**50**:5110-5.

39. Anand R, Gill KD, Mahdi AA. Therapeutics of Alzheimer's disease: Past, present and future. *Neuropharmacol* 2014;**76**:27-50.

40. Delrieu J, Ousset PJ, Caillaud C, Vellas B. Clinical trials in Alzheimer's disease: immunotherapy approaches. *J Neurochem* 2012;**120**:S186-93.

41. Re F, Moresco R, Masserini M. Nanoparticles for neuroimaging. *J Phys D: Appl Phys* 2012;**45**:073001.

Figure Legends

Figure 1. Preparation and characterization of PINPs. **(A)** Amino acid sequence of RI-OR2-TAT. Black letters indicate the RI-OR2 peptide and red letters the TAT sequence, with D-amino acids in lower case. **(B)** Construction of PINPs through 'click' chemistry involving a C-terminal cysteine residue. **(C)** Size distribution of PINPs measured on a Nanosight instrument. **(D)** AFM image of PINPs with no Aβ present.

Figure 2. PINPs are potent inhibitors of $A\beta_{1-42}$ aggregation. All concentrations for PINPs refer to NL-linked inhibitory peptide, to allow comparison with free peptide. **(A)** Time-course of Aβ1-42 aggregation in the presence of non-linked RI-OR2-TAT (1:5 ratio of inhibitor to $A\beta_{1-42}$) or PINPs (1:400, 1:2000 ratio of NL-linked inhibitory peptide to $A\beta_{1-42}$), as determined by ThT assay. **(B)** Dilution series of PINPs against the ThT signal after 48 h incubation. Note that a molar ratio of 1:2000 of NL-linked inhibitory peptide to $A\beta_{1-42}$ (or 1:50 total lipids to $A\beta_{1-42}$) gives ~50% inhibition. **(C)** Data from an immunoassay for oligomeric Aβ. Samples were taken at 0, 2, 4, 8, 12 and 24 h (consecutive bars) from incubations of $A\beta_{1-42}$ alone, or $A\beta_{1-42}$ with 1:40, 1:400, 1:2000 and 1:4000 ratios of NL-linked inhibitory peptide to Aβ.

Figure 3. AFM and EM images confirm that PINPs interact with Aβ and inhibit its aggregation. (A) $A\beta_{1-42}$ at 25 µM was incubated alone for 144 h and examined by AFM. **(B)** Aβ with UD liposomes at a 1:20 ratio of lipids:Aβ. (**C)** Aβ with PINPs at a 1:20 ratio of lipids:Aβ. The presence of fibres (white arrowheads) in **(A)** and **(B)** indicates that UD liposomes do not interfere with Aβ aggregation, whereas **(C)** shows the clear absence of fibrils. PINPs are indicated by the white arrow. **(D)** $A\beta_{1-42}$ incubated with PINPs (4:1 ratio of

lipids:Aβ) and stained with PTA. The PINPs (white arrow) are bound along the length of an amyloid fibril (black arrow) and to its termini. **(E)** 6E10 immunogold labelling of a PINP (grey arrow) following incubation with $A\beta_{1-42}$. White arrows show regions where Aβ was detected. The black arrow shows an Aβ monomer (or small oligomer) labelled with immunogold.

Figure 4. SPR data on binding of PINPs to Aβ fibrils. PINPs were injected at four different concentrations, for 5 min, at a flow rate of 30 µL/min (from bottom to top: 0.3 µM, 0.6 µM, 0.9 µM, 1.2 µM of exposed $A\beta_{1-42}$ peptide). The non-specific binding obtained from the reference surface has been subtracted from all data. Fitted curves are shown in black. The binding affinity (K_d) is calculated as 36-50 nM.

Figure 5. PINPs are not toxic and protect against the damaging effects of Aβ on cells. **(A)** MTS assay data for SHSY-5Y cells grown in the presence of various concentrations (total lipids) of PINPs or UD liposomes. **(B)** LDH assay data for cells exposed to pre-aggregated $A\beta_{1-42}$ (at 5 µM) in the presence or absence of varying concentrations (total lipids) of PINPS or UD liposomes. PINPs protected against the damaging effects of Aβ (* = $p<0.001$). Error bars are too small to be seen.

Figure 6. PINPs can flux across the hCMEC/D3 cell monolayer. 10^6 cells were incubated with UD liposomes (NL) or PINPs radiolabeled with ^{3}H-Sm, for 2 h at 37°C, 5% CO_2. **(A)** Cellular uptake of nanoparticles (NP). After incubation, the amount of ^{3}H-Sm incorporated into the cells was measured and the nmols of total NP taken up by the cells calculated. **(B)** Transcytosis of NP through hCMEC/D3 cell monolayers. Radiolabeled UD liposomes (NL) or PINPs were added to the upper chamber of the transwell monolayers and

incubated for 2 h at 37°C, 5% CO_2. The permeability across the cell monolayer was calculated. Each value is the mean (+/- SD) of at least three independent experiments. * = $p<0.05$ by Student's t-test.

Figure 7. Treatment with PINPs significantly restores long-term recognition memory in Tg2576 mice. WT or Tg2576 mice were treated with PINPs or vehicle and, at the end of treatment, their memory was tested with the NOR test. (**A**) Histograms indicate the time percentage (mean ± SEM) of investigation of the familiar (grey) and novel (black) objects of the experimental groups tested. (**B**) Histograms report the corresponding DI (mean ± SEM). One-way ANOVA, Tukey's post hoc test. *$p<0.05$.

Acknowledgements

The authors thank Pierre-Olivier Couraud from Institut National de la Santé et de la Recherche Médicale (INSERM, Paris, France) for providing the hCMEC/D3 cells.

Table 1. Tissue distribution in CL57/Bl 6 mice using quantitative whole body analysis (QWBA).

Three mice were injected via a tail vein, and a single mouse was sacrificed at 5, 15 and 60 mins post injection. The amount of radioactivity was assessed using QWBA and converted to µg equivalents per gram of tissue (% of total dose/g in brackets).

	µg equivalents of [^{14}C]-Cholesterol PEGylated nanoliposomes per gram of tissue (% of total dose/g)		
	Sample time after injection		
Tissue type	5 minutes	15 minutes	60 minutes
Brain	0.225 (0.415)	0.262 (0.490)	0.182 (0.362)
Liver	6.78 (12.5)	8.36 (15.6)	7.28 (14.5)
Kidney	1.52 (2.80)	1.19 (2.23)	0.889 (1.77)
Lung	32.1† (59.2)	49.4† (92.3)	22.8 (45.5)
Spleen	10.9 (20.0)	16 (29.8)	16 (31.8)
Blood	2.19 (4.04)	0.51 (0.952)	0.36 (0.718)

† Above limit of accurate quantification (>23.5 µg equivalents/g) – extrapolated value reported

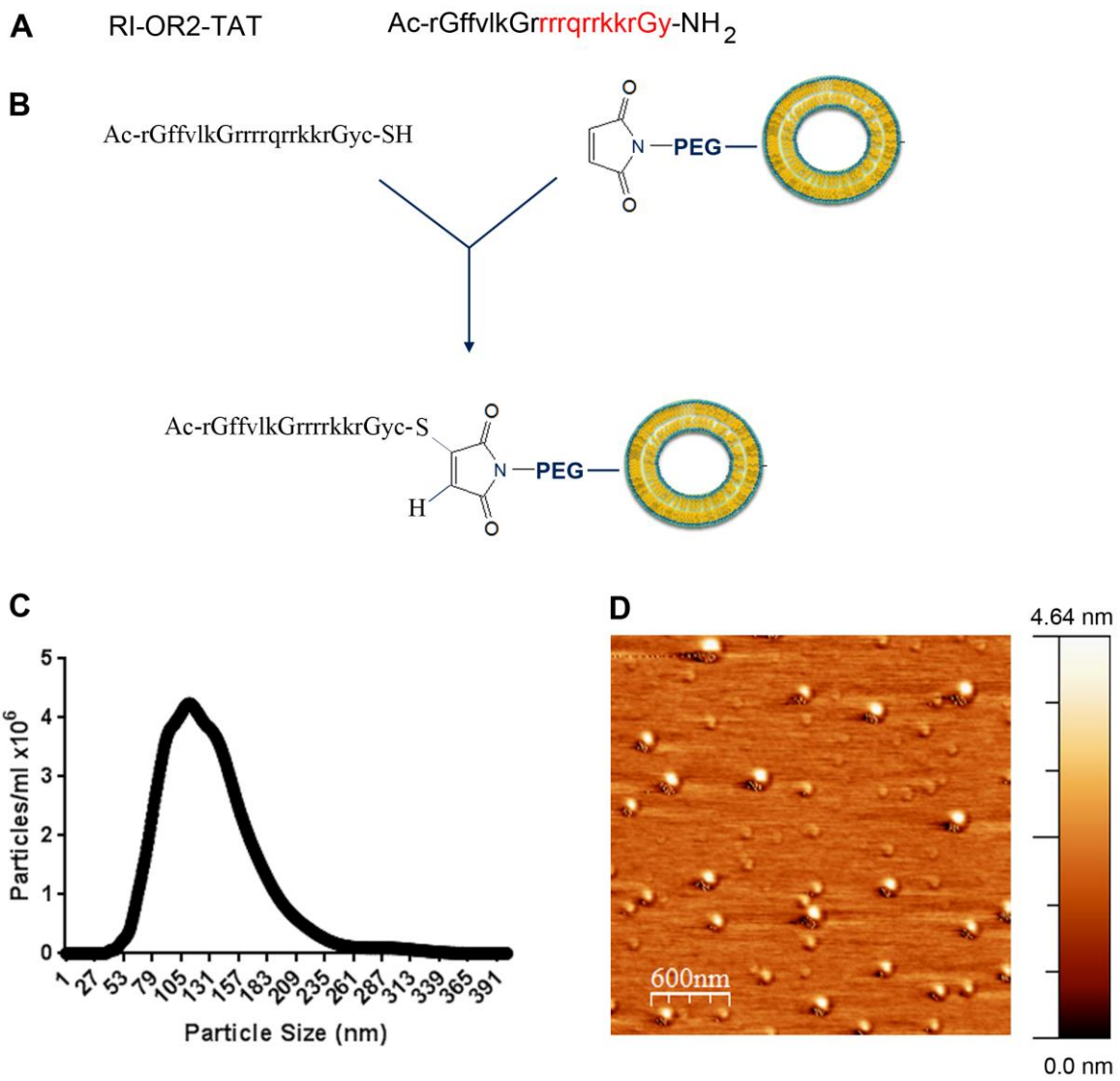

Figure 1

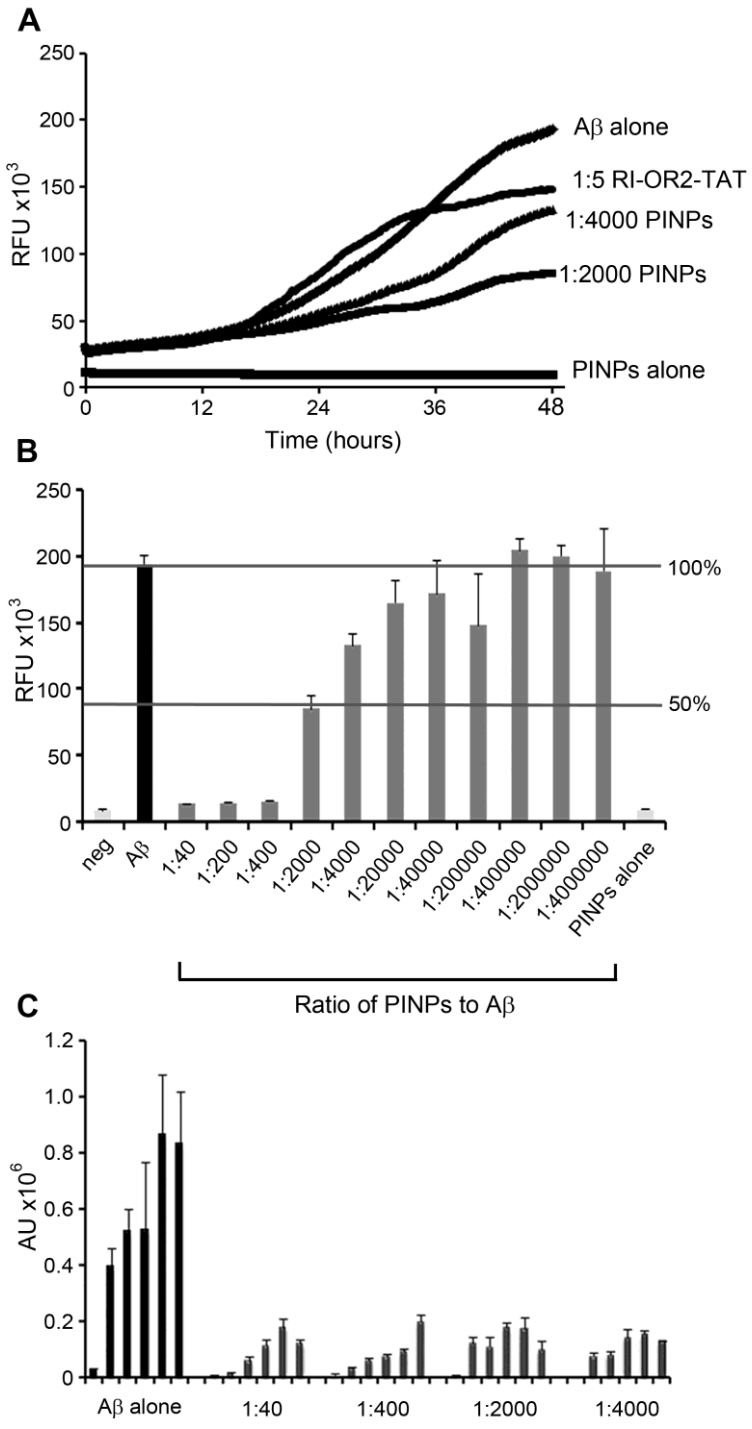

Figure 2

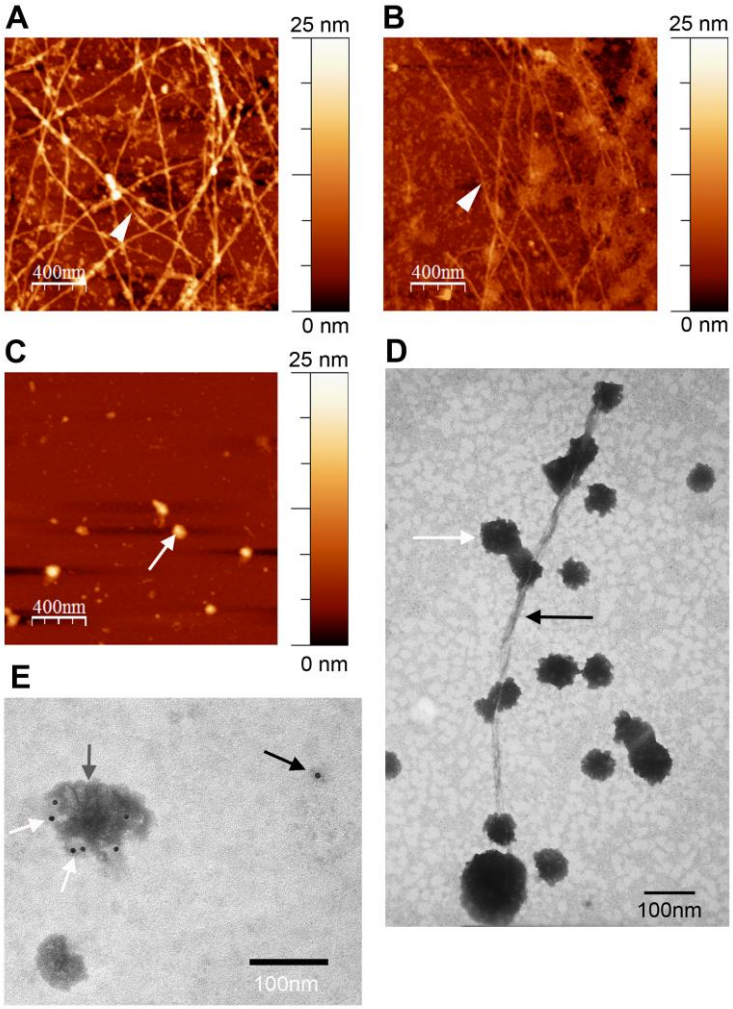

Figure 3

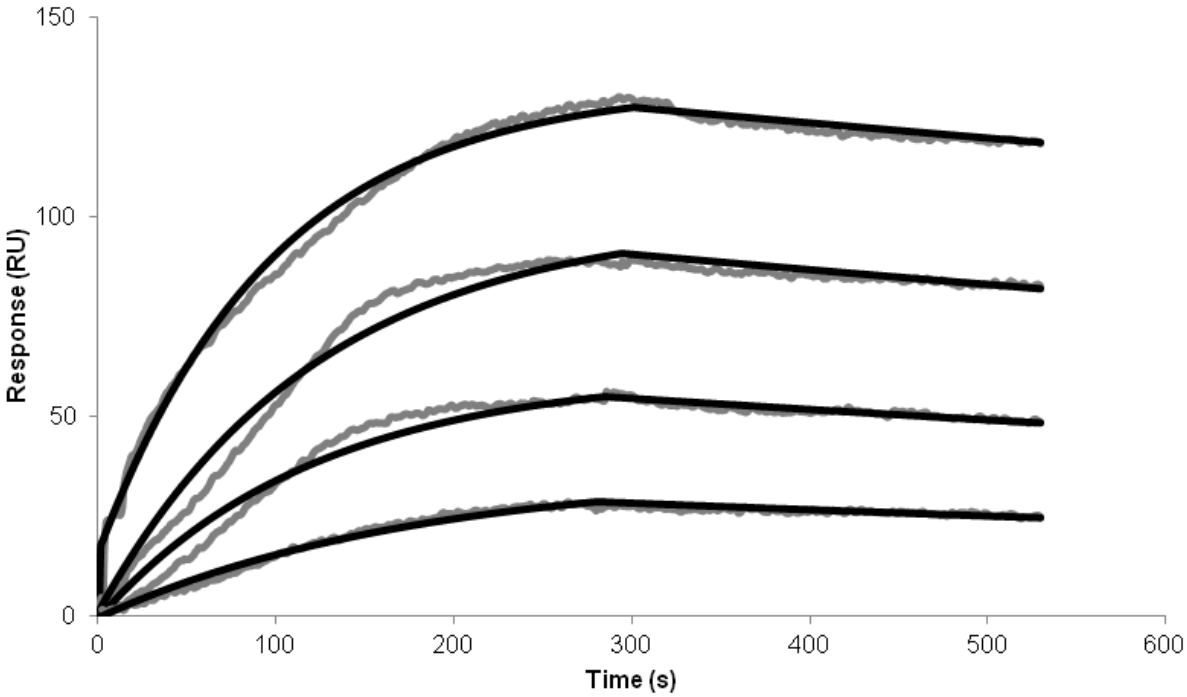

Figure 4

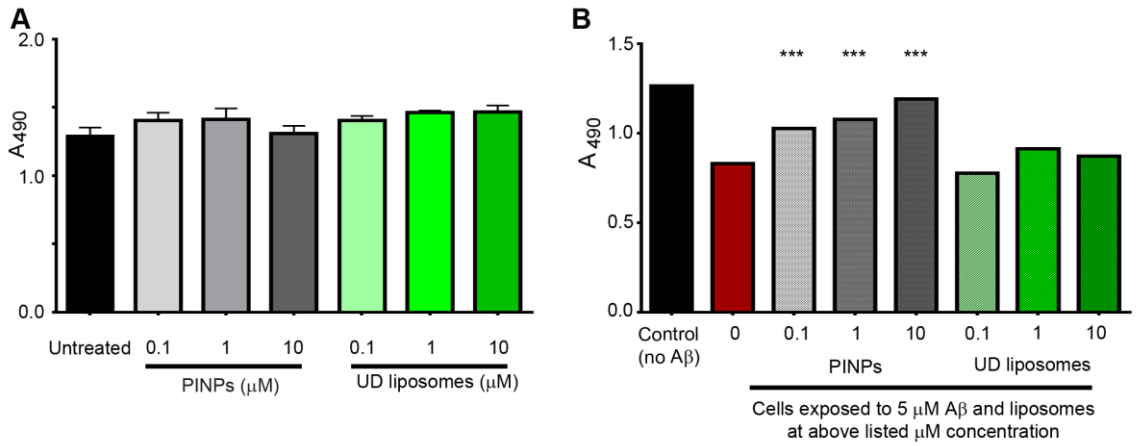

Figure 5

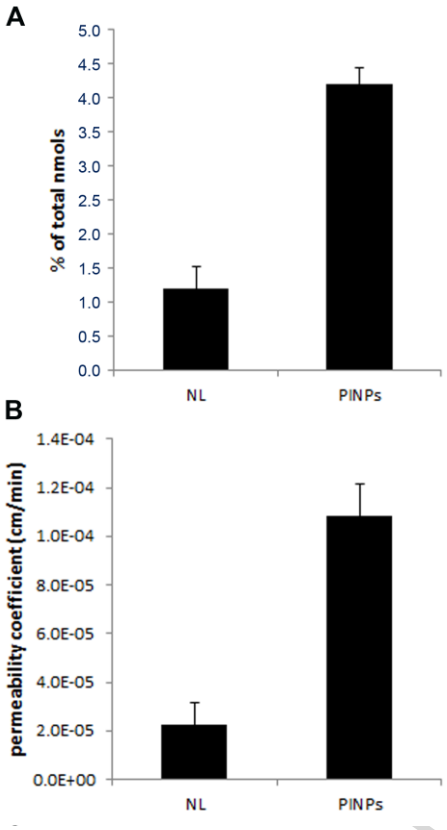

Figure 6

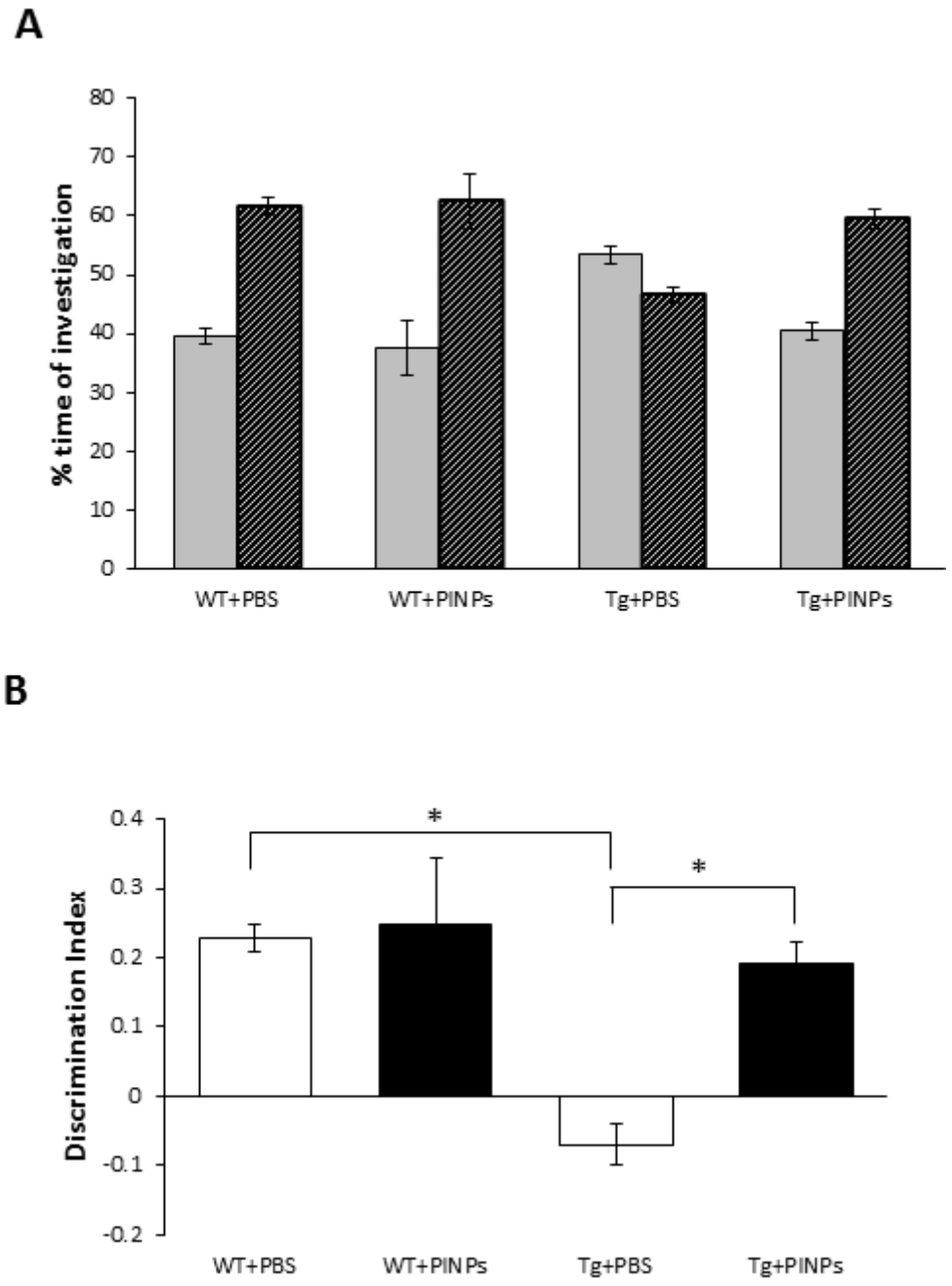

Figure 7

Graphical Abstract

Retro-inverso peptides attached to the surface of nanoliposomes prevent the aggregation of β-amyloid monomers into oligomers and fibrils. The 'ffvlk' sequence of the inhibitory peptide is designed to interact with the 'KLVFF' sequence on the Aβ molecule. However, Aβ could also interact with the positive charge of the 'TAT' sequence and Aβ oligomers, once captured, could insert themselves into the lipid bilayer of the liposomes.